

AD

EDGEOOD ARSENAL TECHNICAL REPORT

SB-TR-75029

02

A METHOD FOR DETERMINING BACKFACE SIGNATURES OF SOFT BODY ARMORS

AD A012797

by

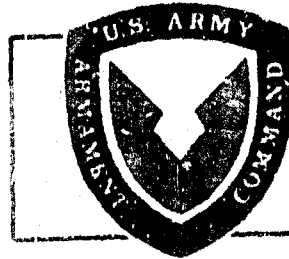
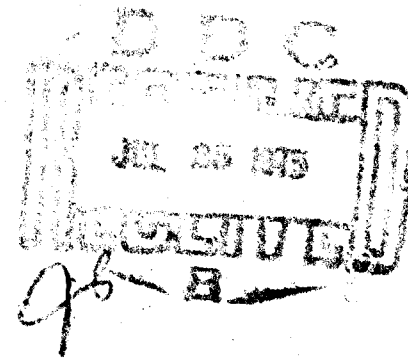
LeRoy W. Metker

Russell N. Prather

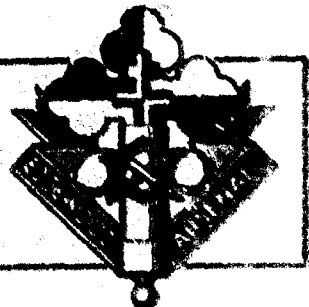
Earl M. Johnson

Biomedical Laboratory

May 1975



DEPARTMENT OF THE ARMY
Headquarters, Edgewood Arsenal
Aberdeen Proving Ground, Maryland 21010



Approved for public release; distribution unlimited.

References

The findings in this report are not to be construed as an official position of the US Department of Defense or the Department of the Army, unless so designated by other authorized documents.

Disposition

Destroy this report when it is no longer needed. Do not return it to the originator.

REPORT DOCUMENTATION PAGE		READ INSTRUCTIONS BEFORE COMPLETING FORM													
1. REPORT NUMBER EB-TR-75029	2. GOVT ACCESSION NO.	3. RECIPIENT'S CATALOG NUMBER													
4. TITLE (and Subtitle) A METHOD FOR DETERMINING BACKFACE SIGNATURES OF SOFT BODY ARMORS,		5. TYPE OF REPORT & PERIOD COVERED Technical Report May 1973-May 1974	6. PERFORMING ORG. REPORT NUMBER												
7. AUTHOR(s) LeRoy W. Metker Russell N. Prather Earl M. Johnson		8. CONTRACT OR GRANT NUMBER(s)													
9. PERFORMING ORGANIZATION NAME AND ADDRESS Commander, Edgewood Arsenal Attn: SAREA-BL-BW Aberdeen Proving Ground, Maryland 21010		10. PROGRAM ELEMENT, PROJECT, TASK AREA & WORK UNIT NUMBERS LEAA-J-IAA-005-4													
11. CONTROLLING OFFICE NAME AND ADDRESS Commander, Edgewood Arsenal Attn: SAREA-TS-R Aberdeen Proving Ground, Maryland 21010		12. REPORT DATE May 1975	13. NUMBER OF PAGES 35												
14. MONITORING AGENCY NAME & ADDRESS (if different from Controlling Office)		15. SECURITY CLASS. (of this report) UNCLASSIFIED													
		15a. DECLASSIFICATION/DOWNGRADING SCHEDULE NA													
6. DISTRIBUTION STATEMENT (of this Report) Approved for public release; distribution unlimited.															
7. DISTRIBUTION STATEMENT (of the abstract entered in Block 20, if different from Report)															
8. SUPPLEMENTARY NOTES															
19. KEY WORDS (Continue on reverse side if necessary and identify by block number) <table style="width: 100%; border-collapse: collapse;"> <tr> <td style="width: 25%;">Backface signature</td> <td style="width: 25%;">Kevlar</td> <td style="width: 25%;">Velocity measurement</td> <td style="width: 25%;">Gelatin</td> </tr> <tr> <td>Transient deformation</td> <td>Blood gases</td> <td>Lung contusion</td> <td>Energy</td> </tr> <tr> <td>Flexible body armor</td> <td>Blunt trauma</td> <td>High-speed photography</td> <td>Ballistics</td> </tr> </table>				Backface signature	Kevlar	Velocity measurement	Gelatin	Transient deformation	Blood gases	Lung contusion	Energy	Flexible body armor	Blunt trauma	High-speed photography	Ballistics
Backface signature	Kevlar	Velocity measurement	Gelatin												
Transient deformation	Blood gases	Lung contusion	Energy												
Flexible body armor	Blunt trauma	High-speed photography	Ballistics												
10. ABSTRACT (Continue on reverse side if necessary and identify by block number) <p>The Law Enforcement Assistance Administration is sponsoring a program to develop improved lightweight, inconspicuous armor that would protect the body from .22-caliber and .38-caliber bullets fired from handguns. Many factors must be considered in the selection of materials to be used in such armor. When high-speed projectiles strike flexible armor materials but do not penetrate, these materials deform quite readily and transmit a large amount of energy to the tissues directly beneath the point of impact. The goal of this study was to develop a method to characterize this deformation or "backface signature" and relate it to tissue damage. Through the use of high-speed photography of backlit gelatin blocks, the backface signatures of the .22-caliber and .38-caliber missiles were defined and related to tissue response. By increasing this data base, a predictive model relating the physical measures of backface signature to the physiological effects could be achieved, greatly reducing the cost of armor evaluation.</p>															

PREFACE

The work described in this report was supported by Contract LEAA-J-IAA-005-4 awarded by the Law Enforcement Assistance Administration, US Department of Justice, under the Omnibus Crime Control and Safe Streets Act of 1968, as amended. This work was started in May 1973 and completed in May 1974. The experimental data are contained in notebooks MN 2549 and MN 1982.

In conducting the research described in this report, the investigators adhered to the "Guide for the Care and Use of Laboratory Animals" as promulgated by the Committee on Revision of the Guide for Laboratory Animals Facilities and Care of the Institute of Laboratory Animal Resources, National Research Council.

The use of trade names in this report does not constitute an official endorsement or approval of the use of such commercial hardware or software. This report may not be cited for purposes of advertisement.

Reproduction of this document in whole or in part is prohibited except with permission of the Commander, Edgewood Arsenal, Attn: SAREA-TS-R, Aberdeen Proving Ground, Maryland 21010; however, DDC and the National Technical Information Service are authorized to reproduce the document for US Government purposes.

Acknowledgments

The authors acknowledge the assistance given by the following individuals: Mr. John J. Holter, who aided in developing the photographic techniques used; Messrs. Robert E. Carpenter, Lyle C. Snyder, and George J. Maschke, who provided ballistics support; Messrs. James L. Thacker and Ernest H. Kandel, who provided electronic support; and Mrs. Myra C. Cohn, who provided extensive data reduction support.

Acknowledgment is also made of the supportive efforts of Messrs. Nickolas Montanarelli and Clarence E. Hawkins, Program Project Officers at Edgewood Arsenal, and of the overall support and administrative guidance received from personnel of the Law Enforcement Assistance Administration, US Department of Justice, particularly Messrs. Joseph Kochanski, Lester Shubin, and George Schollenberger.

CONTENTS

	Page
I. INTRODUCTION	5
II. BACKGROUND	5
A. Test Criteria for Materials	6
B. Protective Material Specifications for Kevlar 29	6
C. Physical Properties of Kevlar 29 Yarn	7
III. EXPERIMENTAL METHODS	8
A. Equipment	8
B. Measurement of Deformation	8
C. Measurement of Deformation Time	8
D. Data Reduction	8
IV. RESULTS	12
V. CONCLUSIONS	26
VI. RECOMMENDATIONS	28
APPENDIX, Ballistic Signature Computer Program	29
DISTRIBUTION LIST	36

LIST OF FIGURES

Figure

1 Experimental Setup	9
2 Deformation-Time History, .22-Caliber Bullet Versus 7-Ply Kevlar 29, 400/2-Denier	10
3 Deformation-Time History, .38-Caliber Bullet Versus 7-Ply Kevlar 29, 400/2-Denier	10
4 Electronic System for Recording Impact Time	11
5 The .38-Caliber Deformation Envelope	18

LIST OF FIGURES (Contd)

Figure		Page
6	Backface Signature Data Applied to the Four-Parameter Lethality Discriminant Model	23
7	Backface Signature Data Applied to the Eight-Parameter Lethality Discriminant Model	23

LIST OF TABLES

Table		
1	Deformation Surface Curves, .38-Caliber, 158-Grain Projectile Versus 7-Ply Kevlar 29, 400/2-Denier	13
2	Deformation Surface Curves, .22-Caliber, 40-Grain Projectile Versus 7-Ply Kevlar 29, 400/2-Denier	14
3	Backface Signature Parameters, .38-Caliber, 158-Grain Projectile Versus 7-Ply Kevlar 29, 400/2-Denier	15
4	Backface Signature Parameters, .22-Caliber, 40-Grain Projectile Versus 7-Ply Kevlar 29, 400/2-Denier	16
5	Backface Signature Parameters, .38-Caliber, 158-Grain Projectile Versus 5-Ply Kevlar 29, 400/2-Denier	17
6	Backface Signature Parameters, .22-Caliber, 40-Grain Projectile Versus 5-Ply Kevlar 29, 400/2-Denier	19
7	Backface Signature Parameters for Various Armor Materials	20
8	Backface Signature Parameters for Unclamped Material	21
9	Average Backface Signature Parameters for Materials Tested Under the Soft Armor Program	22
10	Average Discriminant Parameters for Four-Parameter Model	26
11	Lethality Discriminant Parameters for Eight-Parameter Model	27

A METHOD FOR DETERMINING BACKFACE SIGNATURES OF SOFT BODY ARMORS

I. INTRODUCTION.

This study was undertaken to develop a standard methodology for defining the "backface signature" or behind-the-armor deformation characteristics of missiles impacting upon soft armor materials. The tests were conducted with a new Du Pont material, Kevlar 29. This relatively new soft armor material has an extremely high ratio of tensile strength to areal density, making it an ideal candidate for incorporation into garments where a bulletproof capability is desired. However, soft armor materials such as Kevlar 29 deform quite readily and would, therefore, transmit a great deal of energy to the tissues directly beneath the point of impact.

The goal of this portion of the study was to develop a method to characterize the deformation and relate it to tissue damage or physiological changes in an animal system.

II. BACKGROUND.

The Law Enforcement Assistance Administration under its Equipment Systems Improvement Program is sponsoring a program to develop a lightweight, inconspicuous body armor. Previous work involved indentifying the ballistic qualities of many candidate materials.

The US Army Textile Research Section, Fiber and Fabric Research and Development Branch, Natick Laboratories, Massachusetts, provided technical direction in the selection of ballistic materials to be used in the development of a protective garment. Additional information on protective vests and materials resulted from a survey of the products of the following armor and material manufacturers.

E. I. du Pont de Nemours & Company

Burlington Industrial Fabrics Company

Union Carbide Corporation

Twentieth Century Body Armor

Rolls-Royce Ltd

Imperial Protector Company

Federal Armor Corporation

Second Chance

Protective Materials Company

Fabric Development, Inc.

American Safety Equipment Corporation

Goodyear Aerospace Corporation

Battelle Memorial Institute

Institut de Medecine Legale (Dr. Jan Weinberger)

Franklin Institute Research Laboratories

From this investigation the following materials were selected for testing:

Hi-Tenacity nylon, Du Pont

Hi-Tenacity rayon, Du Pont

Hi-Tenacity dacron, Du Pont

Hi-Tenacity Kevlar 29, Du Pont

Hi-Tenacity Fiber B, Du Pont

Hi-Tenacity Thornel graphite yarn, Union Carbide Corporation

Hi-Tenacity Panex graphite yarn, Union Carbide Corporation & Stackpole, Inc.

Hi-Tenacity X-P, Marlex, Phillips Petroleum Inc.

Hi-Tenacity X-55, Monsanto Company

Standard nylon, Du Pont

Nylon felt, Du Pont

Monsanto X-500 felt, Monsanto Company

A. Test Criteria for Materials.

1. Weight-to-strength ratio: Light in weight but strong enough to defeat penetration of the threat: .38-caliber bullet, 158-grain, at 800 fps; .22-caliber bullet, 40-grain, at 1000 fps.

2. Flexible or nonrigid: Fabric-type material that would allow the wearer freedom of movement.

3. Inexpensive in cost: Adaptable for future law enforcement application.

4. Good ballistic qualities: Ability to absorb energy expended by a bullet that impacts but cannot penetrate.

5. Tailoring: Tailored so as to provide good fit and styled to reduce the appearance of armor.

Using these criteria, test results showed that the Du Pont product, Kevlar 29, was superior to the other materials tested. The initial material chosen as the best candidate armor material was Kevlar 29, 400/2-denier, as specified below.

B. Protective Material Specifications for Kevlar 29.

Style No.	Fabric Development FUSL No. 1 Du Pont TL 105-26
Warp	400 Denier, 267 filaments, 2 plies, 4 twists per inch, Z direction for both longitudinal and filling.
Weave	Plain
Ends per inch	38 ±2
Picks per inch	38 ±2

Weight in ounces per square yard	7.45 ± 0.25 ounces
After fabric is woven, it is scored, rinsed, and dried.	
Width	38.25 inches
Thickness	Approximately 0.015 inch
Current cost	Approximately \$17 per pound for 400 denier

C. Physical Properties of Kevlar 29 Yarn.

Density	1.45 gm/cc	Forty percent lower than glass and boron and slightly lower than graphite.
Tensile strength	400,000 psi	Substantially above conventional organic fibers and equivalent to most high-performance reinforcing fibers.
Specific tensile	8×10^6 inches	Highest of any commercially available reinforcing fibers.
Modulus	19×10^6 psi	Twice that of glass fibers.
Specific modulus	3.5×10^8 inches	Between that of the high modulus graphites and boron and that of glass fibers.
Chemical resistance	Good	Highly resistant to organic solvents, fuels, and lubricants.
Textile processibility	Excellent	Can be readily woven on conventional fabric looms. Retains 90% of its tensile strength after weaving. Can be easily handled on conventional filament winding equipment.
Flammability characteristics	Excellent	Inherently flame-resistant, self-extinguishing when flame source is removed, does not melt.
Temperature resistance	Excellent	No degradation of yarn properties in short-term exposures up to temperatures of 500°F.

Several sample garments have been fabricated from various layers of this material to satisfy user requirements for an inconspicuous, lightweight outer garment, providing protection against .22-caliber and .38-caliber bullets fired from handguns. It has been proposed that sportcoats be fabricated for wear by touring foreign dignitaries, US ambassadors, and other government officials when public exposure is anticipated. There is also an expressed interest by law-enforcement agencies in a similar outer or inner garment that could be incorporated into the standard uniform or used by plainclothes investigators.

III. EXPERIMENTAL METHODS.

A. Equipment.

The initial problem was to develop a method which would allow visualization and measurement of the cone of deformation behind the armor with sufficiently fast response time to allow determination of the loading times or impulse. Several methods of approach were examined to determine the most feasible as well as most cost-effective method.

The results of this study indicated that high-speed photography of backlit gelatin blocks would provide the necessary resolution.

The armor under test was fastened in front of the gelatin block and impacted by the missile, and the event was recorded on high-speed film. The test procedure was the same for all shots.

The test setup is shown in figure 1 and consists of the following: (1) the weapon, a 7-inch, .38-caliber Mann barrel with remote firing capability or a 7-inch, .22-caliber Mann barrel; (2) a 1/2-meter baseline utilizing silver grid screens which activate an electronic chronograph (ECI Model 4600) to measure missile velocity; (3) a Redlake Hycam camera focused on the gelatin-armor interface; (4) a large bank of quartz lights to completely backlight the gelatin block; (5) a steel frame for supporting the armor material; and (6) the armor material. During the actual test operation, the camera is activated; and, when the proper framing rate is achieved, a signal is sent to the firing mechanism to activate the weapon.

B. Measurement of Deformation.

The developed film is processed through a Model 29E Telereadex film analyzer where frame-by-frame measurements of the deformation in the gelatin can be made. Figures 2 and 3 illustrate a typical deformation-time history for each threat against 7 plies of Kevlar 29. Measurements of the depth of penetration as well as the base diameter are made from the point of impact to maximum deformation. Maximum deformation was taken to occur at the point of maximum penetration into the gelatin block. This maximum deformation is then divided into 10 equal parts along the penetration axis and the diameter is measured at each of these points.

C. Measurement of Deformation Time.

The maximum film speed for the Redlake Hycam camera system, approximately 4000 pps, is too slow to permit precise measurement of the deformation time. In an attempt to more accurately define this time interval, an electronic system was developed for recording on the film the incidence of missile impact upon the sample. The components of this system are shown in figure 4 and function in the following manner: (1) an additional chronograph (Monsanto Model L101C), connected to the velocity measurement screens, records the missile transit time through these screens. This time interval is then programmed into (2) a digital comparator (Monsanto Model 504A). The stop signal into the L101C chronograph also generates a start signal into (3) a preset/variable time base counter (Monsanto Model 104B) which also connects to the digital comparator. When the time on the Model 104B coincides with that programmed into the digital comparator, the comparator generates a signal which fires a pulser. This pulser in turn triggers a modified time delay generator, dimming an extra timing light installed for this purpose into the Redlake camera. Thus a record of the impact time was placed on the film since the sample under test was the same distance from the stop screen as the distance between the velocity measurement screens.

D. Data Reduction.

Analysis of the film on the Telereadex system led to an accurate measurement of the film framing rate. This film speed, when used in conjunction with the number of frames of deformation, the physical dimension of the film frame, and the recorded time of impact, led to a more precise definition of the deformation time interval by halving the measurement error from ± 1 frame to $\pm 1/2$ frame (approximately $\pm 150 \mu\text{sec}$).

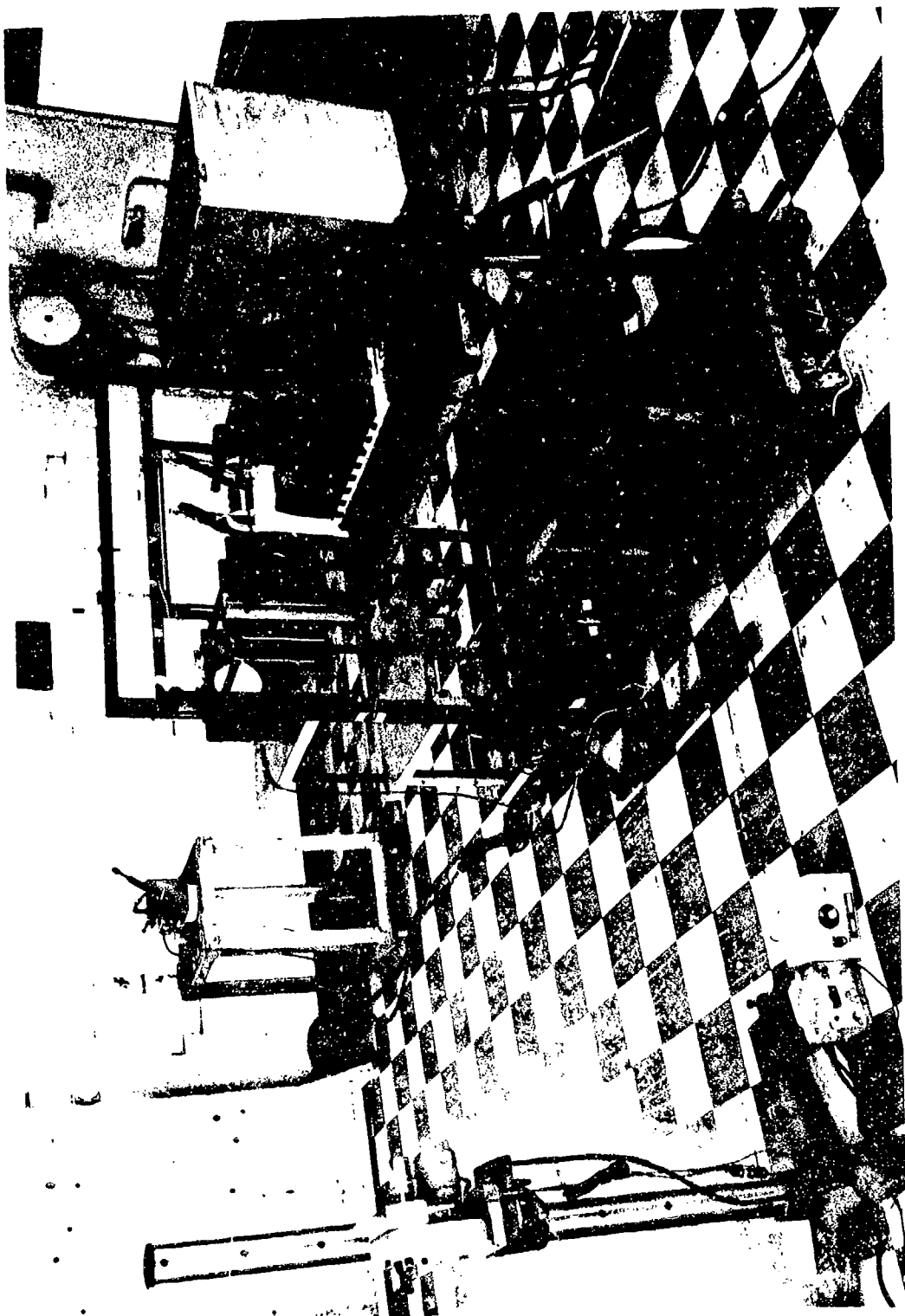


Figure 1. Experimental Setup

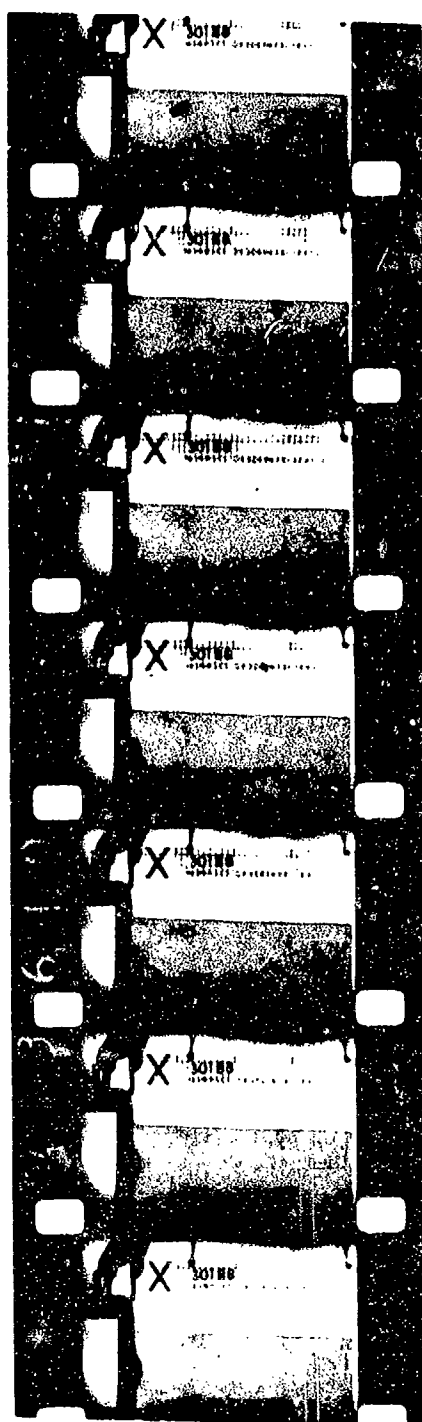


Figure 2. Deformation-Time History, .22-Caliber Bullet Versus 7-Ply Kevlar 29, 400/2-Denier

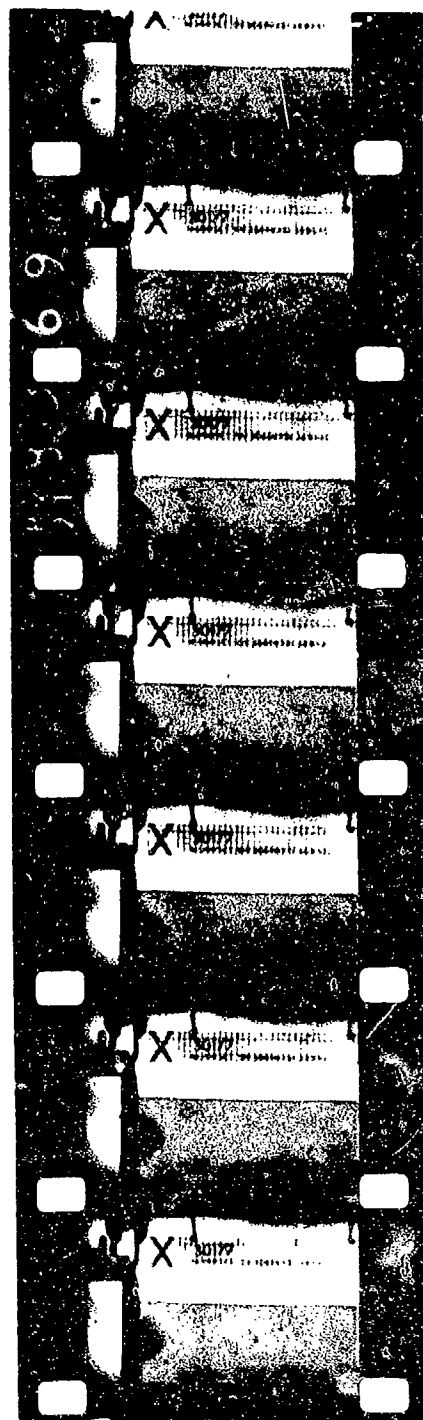


Figure 3. Deformation-Time History, .38-Caliber Bullet Versus 7-Ply Kevlar 29, 400/2-Denier

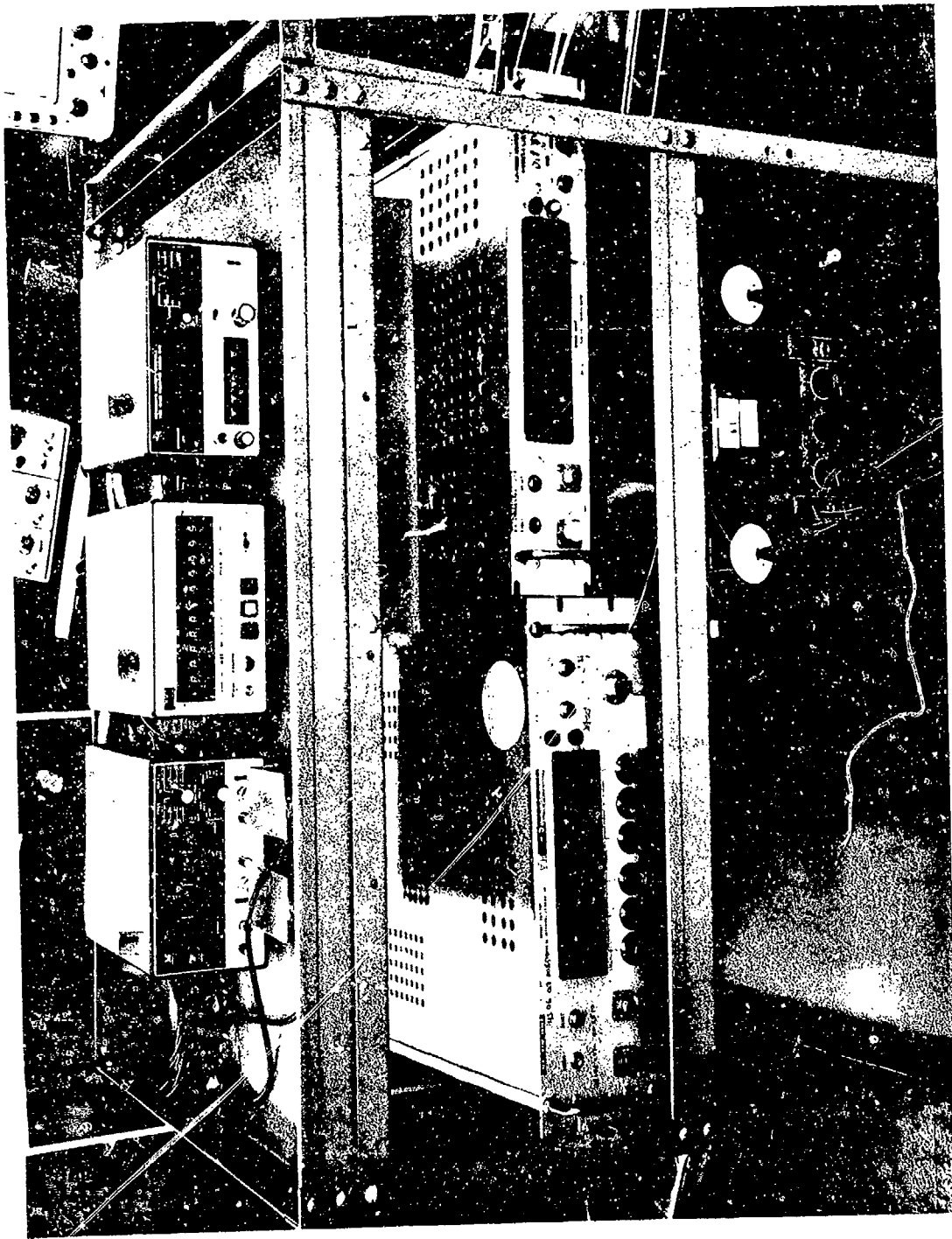


Figure 4. Electronic System for Recording Impact Time

The data acquired from the film analysis, in machine counts, was then processed on a Univac 1108 computer through the computer program shown in the appendix. This program processes the data in the following manner:

1. The Telereadex data in machine counts is converted to centimeter by using a conversion factor obtained from each film.

2. The depth of penetration and the maximum deformation radius per frame are listed.

3. The average velocity of deformation $\left(\frac{\text{penetration per frame}}{\text{time interval per frame}} \right)$ is listed.

4. The maximum deformation, defined by 10 equidistant points along the axis of penetration and their associated radii of deformation, is computed and listed.

5. The maximum deformation data can then be run through a series of equations to determine a general curve which best describes the deformation surface. This general analysis was performed on some of the initial backface signature measurements and the best fit was determined to be of the form

$$y^2 = a + bx$$

where

y = deformation radius

x = depth of penetration

a, b = regression constants

This form was then used for all subsequent deformation characterizations. An initial assumption was made that the deformation being measured was symmetrical. Castings made from deformations in clay have verified that this assumption is realistic.

6. The program then calculates and lists a deformation volume which is derived by revolving the parabolic curve about the axis of penetration and generating a paraboloid of revolution. If $y^2 = a + bx$, then $A(x) = \pi y^2 = \pi(a + bx)$, and $V = \int_0^x A(x) dx = \pi x(a + bx/2)$.

IV. RESULTS.

The equations for the regression fit curves defining the maximum deformation of 7 plies of 400/2-denier Kevlar 29 material in gelatin along with their associated correlation coefficients and root mean square values are listed in table 1 for the .38-caliber threat and in table 2 for the .22-caliber threat. Tables 3 and 4 list the impact velocities, calculated deformation volumes, deformation times, and measured maximum depths of penetration for the .38-caliber and .22-caliber threats, respectively. The upper and lower bounds for the .38-caliber deformations in gelatin are shown in figure 5, in which x is the penetration axis and y is the axis along which the base diameters were measured. The dashed curve in figure 5 represents the average .38-caliber deformation curve.

Backface signature data for 5 plies of Kevlar 29 are presented in table 5 for the .38-caliber bullet and in table 6 for the .22-caliber bullet. These data were acquired during the initial phase of the program while the test methodology was being established. It is important to note that the .22-caliber velocities are substandard; i.e., 800 fps as opposed to the recommended test velocity of 1000 fps. These tests were conducted prior to the establishment of the 1000-fps test velocity. Furthermore, the surface equations are not computer fits as established for the 7-ply Kevlar 29; they are calculated equations for parabolic surfaces, $y^2 = cx$, using the diameter/depth ratios to determine the constant c .

Table 1. Deformation Surface Curves
.38-Caliber, 158-Grain Projectile Versus 7-Ply Kevlar 29, 400/2-Denier

Film No.	Deformation surface	Correlation coefficient	Root mean square
30008	$y^2 = 22.21 - 4.9496x$	0.9926	0.1745
30177	$y^2 = 21.37 - 4.3428x$	0.9770	0.2303
30178	$y^2 = 26.94 - 5.6105x$	0.9898	0.2828
30179	$y^2 = 20.14 - 4.2740x$	0.9912	0.1583
30180	$y^2 = 18.71 - 4.1402x$	0.9812	0.2161
30181	$y^2 = 22.57 - 4.9741x$	0.9937	0.1531
30182	$y^2 = 17.52 - 3.9631x$	0.9855	0.1744
30183	$y^2 = 20.47 - 4.7358x$	0.9915	0.1659
30184	$y^2 = 21.97 - 4.5600x$	0.9967	0.0962
30185	$y^2 = 20.53 - 4.2851x$	0.9900	0.1948
30186	$y^2 = 20.63 - 4.6267x$	0.9916	0.1589
30187	$y^2 = 17.73 - 4.8461x$	0.9896	0.1946
30318	$y^2 = 26.56 - 6.3305x$	0.9759	0.2485
30319	$y^2 = 19.38 - 4.3465x$	0.9830	0.2023
30320	$y^2 = 18.16 - 3.8933x$	0.9746	0.2156
30321	$y^2 = 18.61 - 4.6926x$	0.9820	0.1932
30322	$y^2 = 21.02 - 5.0760x$	0.9925	0.1406

Table 2. Deformation Surface Curves

.22-Caliber, 40-Grain Projectile Versus 7-Ply Kevlar 29, 400/2-Denier

Film No.	Deformation surface	Correlation coefficient	Root mean square
30022	$y^2 = 14.25 - 5.6138x$	0.9923	0.0982
30188	$y^2 = 8.12 - 3.7612x$	0.9851	0.2006
30189	$y^2 = 12.00 - 4.8772x$	0.9888	0.1306
30190	$y^2 = 6.58 - 2.2654x$	0.9818	0.1182
30191	$y^2 = 11.00 - 4.2342x$	0.9885	0.1971
30194	$y^2 = 7.57 - 2.8941x$	0.9901	0.1379
30195	$y^2 = 16.44 - 5.1773x$	0.8528	0.6302
30196	$y^2 = 6.44 - 2.9744x$	0.9830	0.1429
30197	$y^2 = 16.68 - 7.8952x$	0.9428	0.3281
30198	$y^2 = 10.33 - 3.8922x$	0.9898	0.1494
30199	$y^2 = 8.76 - 3.2425x$	0.9938	0.1166
30329	$y^2 = 9.32 - 3.2120x$	0.9800	0.1798
30330	$y^2 = 9.80 - 3.4865x$	0.9918	0.1130
30331	$y^2 = 7.58 - 2.5134x$	0.9571	0.1878
30353	$y^2 = 9.77 - 4.1922x$	0.9932	0.0834

Table 3. Backface Signature Parameters
.38-Caliber, 158-Grain Projectile Versus 7-Ply Kevlar 29, 400/2-Denier

Film No.	Striking velocity	Maximum volume	Maximum depth	Maximum base radius	Deformation time
	m/sec	cc	cm	cm	sec
30008	243.7	155.69	4.82	4.76	0.0017
30177	253.9	165.15	4.99	4.12	0.0018
30178	255.4	202.07	5.17	5.18	0.0018
30179	249.6	148.51	5.00	4.61	0.0021
30180	247.8	132.50	4.72	4.01	0.0018
30181	249.3	159.95	4.88	4.99	0.0018
30182	251.5	121.50	4.60	3.79	0.0016
30183	249.0	138.26	4.64	4.60	0.0018
30184	259.1	165.86	5.08	4.79	0.0015
30185	254.8	153.35	5.20	4.62	0.0021
30186	255.4	143.60	4.80	4.97	0.0016
30187	254.5	101.12	3.98	4.50	0.0016
30318	249.8	172.66	4.65	4.91	0.0015
30319	246.8	134.97	4.71	3.99	0.0014
30320	247.3	132.94	4.84	3.77	0.0016
30321	245.9	115.77	4.14	3.84	0.0013
30322	248.1	136.24	4.42	4.45	0.0015
Mean	250.7	145.89	4.74	4.46	0.0017
Standard deviation	4.17	23.89	0.33	0.46	0.0002

Table 4. Backface Signature Parameters
.22-Caliber, 40-Grain Projectile Versus 7-Ply Kevlar 29, 400/2-Denier

Film No.	Striking velocity	Maximum volume	Maximum depth	Maximum base radius	Deformation time
	m/sec	cc	cm	cm	sec
30022	318.3	56.42	2.75	3.95	0.0012
30188	305.2	27.49	2.10	5.40	0.0012
30189	310.0	45.94	2.70	3.52	0.0008
30190	317.9	29.67	3.24	2.48	0.0008
30191	306.1	44.38	2.87	3.17	0.0010
30194	307.9	31.13	2.58	2.50	0.0008
30195	310.8	77.07	3.95	5.31	0.0010
30196	309.6	21.88	2.22	2.34	0.0008
30197	303.0	53.95	2.45	4.63	0.0010
30198	306.0	43.07	2.69	2.99	0.0010
30199	307.5	37.17	2.78	2.86	0.0011
30329	310.7	42.46	2.92	2.70	0.0008
30330	315.3	43.23	2.93	2.84	0.0008
30331	303.8	35.89	3.03	2.34	0.0007
30333	306.0	35.69	2.44	2.92	0.0006
Mean	309.2	41.70	2.78	3.33	0.0009
Standard deviation	4.78	13.60	0.44	1.03	0.0002

Table 5. Backface Signature Parameters
.38-Caliber, 158-Grain Projectile Versus 5-Ply Kevlar 29, 400/2-Denier

Film No.	Striking velocity	Surface equation	Maximum volume	Maximum depth	Maximum base radius	Deformation time
	m/sec		cc	cm	cm	sec
29966	246.1	$y^2 = 3.23x$	149.60	5.4	4.19	0.0020
29967	244.0	$y^2 = 3.84x$	155.05	5.07	4.41	0.0017
29968	241.4	$y^2 = 4.13x$	183.61	5.32	4.69	—
29969	248.0	$y^2 = 4.21x$	162.69	4.96	4.57	0.0014
29970	249.8	$y^2 = 4.80x$	172.27	4.78	4.79	0.0014
29971	247.6	$y^2 = 3.46x$	97.71	4.24	3.83	0.0012
29972	242.4	$y^2 = 4.36x$	137.46	4.48	4.42	0.0012
29973	249.9	$y^2 = 4.61x$	160.64	4.71	4.66	0.0017
29974	247.5	$y^2 = 4.14x$	140.61	4.65	4.39	0.0015
29975	243.1	$y^2 = 3.72x$	105.05	4.24	3.97	0.0015
29976	248.6	$y^2 = 3.36x$	111.68	4.60	3.93	0.0014
29977	247.3	$y^2 = 2.98x$	114.23	4.94	3.84	—
29979	247.6	$y^2 = 3.04x$	133.63	5.29	4.01	0.0014
Mean	246.4		140.33	4.82	4.28	0.0015
Standard deviation	2.8		26.96	0.39	0.34	0.0002

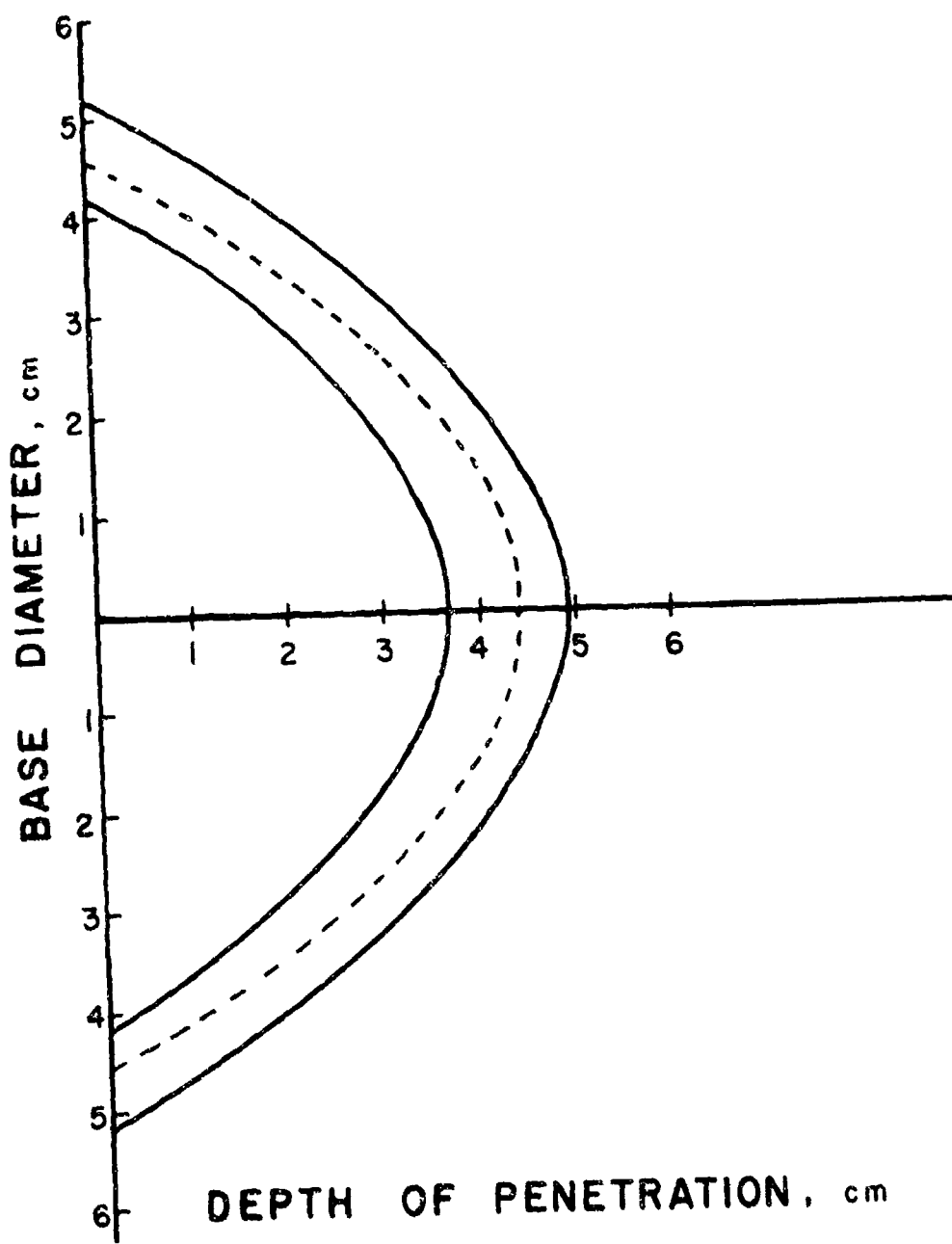


Figure 5. The .38-Caliber Deformation Envelope

Table 6. Backface Signature Parameters
.22-Caliber, 40-Grain Projectile Versus 5-Ply Kevlar 29, 400/2-Denier

Film No.	Striking velocity	Surface equation	Maximum volume	Maximum depth	Maximum base radius	Deformation time
	m/sec		cc	cm	cm	sec
29980	251.6	$y^2 = 4.14x$	37.77	2.41	3.16	0.0014
29981	233.1	$y^2 = 2.35x$	34.1	3.04	2.67	0.0014
29982	230.5	$y^2 = 2.64x$	18.11	2.09	2.35	
29983	237.6	$y^2 = 3.52x$	23.69	2.07	2.70	0.0009
29985	239.1	$y^2 = 2.68x$	14.25	1.84	2.22	0.0009
29986	228.7	$y^2 = 2.54x$	20.56	2.27	2.40	0.0009
29988	251.3	$y^2 = 2.60x$	24.31	2.44	2.52	0.0011
29989	242.7	$y^2 = 3.90x$	31.45	2.24	2.99	0.0009
29991	262.5	$y^2 = 2.64x$	25.92	2.50	2.57	0.0011
29992	231.8	$y^2 = 2.37x$	25.17	2.60	2.48	0.0011
29993	231.9	$y^2 = 2.09x$	23.40	2.67	2.36	0.0011
29994	248.6	$y^2 = 2.28x$	19.95	2.36	2.32	0.0009
29995	232.1	$y^2 = 2.82x$	26.16	2.43	2.62	0.0006
Mean		240.1	24.99	2.38	2.57	0.0010
Standard deviation		10.5	6.47	0.30	0.27	0.0002

Other materials given limited testing under this program were: 7 plies of 200-denier Kevlar 29, 7 plies of 400/2-denier Kevlar 29 subjected to water immersion, freezing at -26°F for 50 hours and thawed before test (part of the simulated aging process), and 12 plies of ballistic nylon. The results of these tests are listed in table 7.

Limited testing was conducted to determine the effect of clamping the material. Both 5 and 7 plies of Kevlar 29 were tested in an unclamped state. The results, listed in table 8, indicate that clamping produced no significant effect for the deformation times realized in these ballistic tests. This may not be true for deformation of longer time duration.

Table 9 summarizes the data acquired under this part of the study as well as that derived from the material matrix test.

Modeling.

Illustrated in figures 6 and 7 are two proposed blunt trauma models for thoracic impacts described in a report on blunt trauma correlation.*

* Clare, Victor R., Lewis, James H., Mickiewicz, Alexander P., and Sturdivan, Larry M. EB-TR-75016. Blunt Trauma Data Correlation. May 1975.

Table 7. Backface Signature Parameters for Various Armor Materials

Film No.	Material	Missile	Striking velocity	Surface equation	Maximum volume	Maximum depth	Maximum radius	Deformation time
			m/sec		cc	cm	cm	sec
30347	7-Ply, 200-denier	.38	258.1	$y^2 = 21.97 - 3.995x$	189.51	5.61	4.17	0.0017
30348	7-Ply, 200-denier	.38	258.5	$y^2 = 21.44 - 3.8224x$	188.88	5.63	4.12	0.0017
30349	7-Ply, 200-denier	.38	262.9	$y^2 = 23.33 - 4.2692x$	200.05	5.64	4.33	0.0018
30350	7-Ply, 200-denier	.38	258.3	$y^2 = 20.25 - 3.6799x$	174.76	5.75	4.21	0.0016
30351	7-Ply, 200-denier	.38	254.0	$y^2 = 23.13 - 4.2410x$	197.97	5.62	4.29	0.0019
30352	7-Ply, 200-denier	.38	254.1	$y^2 = 22.56 - 4.7012x$	169.90	4.93	4.35	0.0016
30353	7-Ply, 200-denier	.38	257.8	$y^2 = 19.61 - 3.6335x$	166.00	5.57	4.16	0.0015
30354	7-Ply, 200-denier	.38	254.7	$y^2 = 19.36 - 3.9316x$	149.66	5.07	3.94	0.0013
30355	7-Ply, 200-denier	.38	257.6	$y^2 = 21.17 - 4.0655x$	172.99	5.35	4.16	0.0018
Mean			257.3		178.86	5.46	4.19	0.0017
Standard deviation			2.8		16.50	0.29	0.13	0.0002
30369	12-Ply Nylon	.38	248.6	$y^2 = 23.20 - 6.9878x$	120.36	3.09	4.21	0.0014
30370	12-Ply Nylon	.38	243.1	$y^2 = 27.94 - 8.4263x$	145.38	3.21	4.65	0.0017
30371	12-Ply Nylon	.38	242.5	$y^2 = 21.33 - 6.1790x$	115.05	3.21	4.29	0.0012
30372	12-Ply Nylon	.38	248.6	$y^2 = 17.47 - 5.7816x$	82.75	2.90	3.76	0.0012
Mean			245.70		115.88	3.10	4.23	0.0014
Standard deviation			3.4		25.75	0.15	0.37	0.0002
3031A	7-Ply Kevlar 29, frozen and thawed	.38	255.6	$y^2 = 34.82 - 7.0177x$	271.23	5.08	5.18	0.0014
3032A	7-Ply Kevlar 29, frozen and thawed	.38	257.5	$y^2 = 22.13 - 5.1700x$	148.76	4.36	4.19	0.0012
3033A	7-Ply Kevlar 29, frozen and thawed	.38	250.9	$y^2 = 23.37 - 5.5706x$	153.77	4.37	4.28	0.0016
3034A	7-Ply Kevlar 29, frozen and thawed	.38	-	$y^2 = 22.49 - 5.4874x$	143.63	4.46	4.41	0.0010
Mean			254.7		179.35	4.57	4.52	0.0013
Standard deviation			3.4		61.39	0.34	0.45	0.0003

Table 7. Contd

Film No.	Material	Missile	Striking velocity	Surface equation	Maximum volume	Maximum depth	Maximum radius	Deformation time
30358	7-Ply, 200-denier	.22	301.9	$y^2 = 9.24 - 3.3033x$	40.49	2.65	2.76	0.0009
30359	7-Ply, 200-denier	.22	310.1	$y^2 = 7.88 - 3.0665x$	31.79	2.58	2.49	0.0009
30360	7-Ply, 200-denier	.22	315.7	$y^2 = 8.37 - 3.4153x$	32.19	2.56	2.63	0.0009
30361	7-Ply, 200-denier	.22	301.3	$y^2 = 8.74 - 3.1045x$	38.61	2.81	2.62	0.0012
30362	7-Ply, 200-denier	.22	311.6	$y^2 = 8.47 - 3.0152x$	37.35	2.72	2.54	0.0009
30364	7-Ply, 200-denier	.22	309.6	$y^2 = 5.35 - 2.8219x$	15.80	2.08	2.41	0.0006
30365	7-Ply, 200-denier	.22	320.7	$y^2 = 9.41 - 3.5060x$	39.64	2.71	2.81	0.0009
Mean			310.1		33.70	2.60	2.61	0.0009
Standard deviation			7.0		8.61	0.25	0.14	0.0002

Table 8. Backface Signature Parameters for Unclamped Material

Film No.	Material	Missile	Striking velocity	Surface equation	Maximum volume	Maximum depth	Maximum radius	Deformation time
29978	5-Ply, 400/2-denier	.38	246.8	$y^2 = 3.94x$	189.95	5.54	4.67	-
30366	7-Ply, 400/2-denier	.38	249.4	$y^2 = 14.22 - 2.8301x$	111.74	5.38	3.59	0.0014
30373	7-Ply, 200-denier	.38	254.5	$y^2 = 14.26 - 3.1819x$	99.26	4.97	3.35	0.0017

Table 9. Average Backface Signature Parameters for Materials Tested Under
the Soft Armor Program

Missile		Material	Ply	Striking velocity	Maximum depth	Maximum volume	Deformation time
Caliber	Weight						
.22	40	grains		m/sec	cm	cc	sec
			5	240.1	2.38	24.99	0.0010
			7	309.2	2.78	41.70	0.0009
			15*	310.8	2.02	29.02	0.0016
			7	310.1	2.60	33.70	0.0008
			3*	247.5	6.78	203.43	0.0020
			5	246.3	4.89	140.33	0.0015
			7	250.7	4.74	145.89	0.0017
			9*	241.9	4.53	166.90	0.0019
			15*	247.9	4.08	176.78	0.0020
			23*	248.5	5.38	113.07	0.0025
.38	158	Kevlar 29, 400/2-denier					
			7	257.3	5.46	178.86	0.0017
			12	245.7	3.10	115.89	0.0014
.45	234	Kevlar 29, 400/2-denier (aged)					
			7	254.7	4.57	179.35	—
			7	242.1	5.32	210.3	0.0017
9-mm	124	Kevlar 29, 400/2-denier w/13.2 oz/square feet XP	7*	370.1	3.72	189.5	0.0017
			23*	322.8	3.66	93.95	0.0017

* One round.

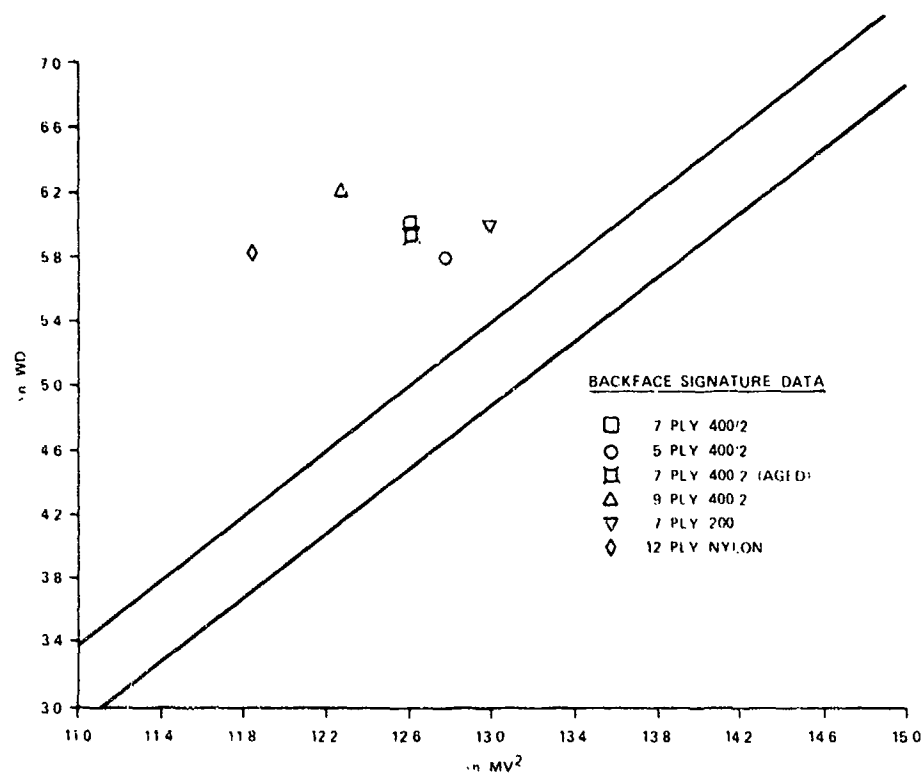


Figure 6. Backface Signature Data Applied to the Four-Parameter Lethality Discriminant Model

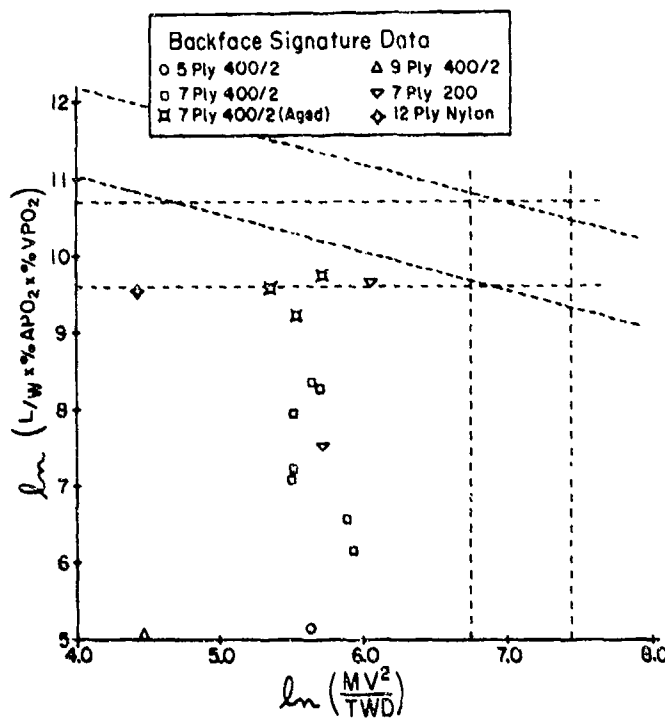


Figure 7. Backface Signature Data Applied to the Eight-Parameter Lethality Discriminant Model

The first model, a four-parameter discriminant model, utilizes the maximum number of parameters common to all the published data sets examined. This model accomplishes its discrimination in a plane whose axes x_1 , x_2 are defined by

$$x_1 = \ln [MV^2]$$

$$x_2 = \ln [WD]$$

where

M = projectile mass (grams)

V = projectile impact velocity (meters per second)

W = experimental animal body weight (kilograms)

D = projectile diameter (centimeters)

The discriminant lines establish three zones of low, mid, and high lethality; i.e., as the impact dose increases, the probability of lethality should also increase for targets having the same body weight and for projectiles of the same diameter.

The second model, involving eight parameters, provides better live/die discrimination than the four-parameter model. This model (figure 7) also accomplished its discrimination in a plane whose axes y_1 , y_2 are defined by

$$y_1 = \ln (MV^2/TWD)$$

$$y_2 = \ln [(L/W)(\%APO_2)(\%VPO_2)]$$

where

M, V, W, and D = same as in the four-parameter model,

T = tissue thickness (centimeters) over the vital organ impacted

L = the total animal lung weight (grams)

%APO₂ = maximum deviation in arterial oxygen pressure from control value

%VPO₂ = maximum deviation in venous oxygen pressure from control value

As in the four-parameter model, the discriminant lines establish zones of negative, mixed, and positive response for a live/die criterion.

These models were formulated from experimental data sets obtained from tests on unarmored animals for which the physical characteristics of the impacting projectile (mass, velocity, diameter) were known. High-mass (50 to 200 grams), low-velocity projectile impacts were involved. Upon formulation of these models, it was proposed that the backface signature be characterized in such a manner that it could be applied to these models. By using this predictive capability and determining in the nonlethal area the degree of decreasing injury potential with decreasing ordinate or "dose" levels, an analysis of the backface signature alone would provide an initial estimate of a candidate armor materials's worth, thereby precluding extensive and costly animal testing.

Conditions comparable to those found in these models occur in armor tests when the primary impactor is taken to be that of the missile-material interaction. However, as the armor deforms under nonpenetrating impact, the impactor mass and velocity are changing with time; i.e., the mass is increasing and the velocity is decreasing until at some time "t", depending on the armor deformation characteristics and the tissue response, maximum deformation mass is achieved. At this same point in time, the velocity of the impactor is zero. Thus, a more extensive analysis of the backface signature than that thus far presented is necessary to conform armor deformation to the physical doses used in the models. This was accomplished in the following manner:

1. Velocity.

By employing the principle of the conservation of linear momentum, a pseudo-velocity for the armor deformation was derived:

$$M_p V_p = (M_A + M_p) V$$

$$V = M_p V_p / (M_A + M_p)$$

where

M_p , V_p = the initial mass (kilograms) and velocity (meters per second) of the impacting projectile

M_A = the armor deformation mass (kilograms)

V = the "effective" armor velocity (meters per second)

2. Mass.

The mass used in applying the soft armor deformation to the models was the projectile-armor mass involved in the maximum deformation. As a conservative approach, the armor mass was assumed to be the mass derived by using the base of the deformation cone; i.e.,

$$M_A = (A_B) (a.d.)$$

A_B = the base area of the deformation surface (square centimeters)

a.d. = the areal density of the armor material (grams per square centimeter)

This estimate is conservative in that the models employ an energy term, MV^2 , and the armor mass is used to determine the "effective" velocity behind the armor. If the entire surface mass had been used, a smaller "effective" velocity would then be derived and hence a smaller dose level would be predicted. Furthermore, it is not known at this time whether the armor mass involved in the deformation is due solely to material elongation, slack in sample mounting, or a combination of the two.

The measurement of the necessary postexperimental parameters required for use in the model is straightforward and is described in the following text. For the modeling of the physiological response of the test animals, several design constraints were established. The animal target is, of course, a combination of many systems and subsystems and the monitoring of all of these would be an impossible task. Targeting, therefore, was restricted initially to one target organ and monitoring to one physiological system. The system chosen was the respiratory system, and the target organ was, of course, the lung. This choice allowed a large target area and provided a system which could be monitored continuously with minimal surgical intervention and relatively simple instrumentation.

The animals used in this study were castrated male angora goats weighing approximately 40 kg. The animals were premedicated with 20 mg of acepromazine and then anesthetized intravenously with sodium pentobarbital. An endotracheal tube was inserted to insure a patent airway and prevent the aspiration of fluids. Catheters were inserted in the left carotid artery and the left jugular vein for blood sampling during the experiment.

Anesthesia was stringently controlled so that the animal's arterial oxygen tension was above 80 mmHg prior to impact. The anesthetized animals were suspended on a specially designed cart, armored with the Kevlar material, and impacted over the designated target area. Arterial and venous blood samples were drawn at 15, 30, and 60 minutes after impact for blood gas analysis. Samples were again drawn at 24 hours and the animals were sacrificed. A complete necropsy was performed and precise measurements were taken of all lesions produced. Of the many parameters measured, four are currently being used in the analysis: arterial oxygen tension, venous oxygen tension, lung weight, and total body weight. These are the postexperimental parameters shown on the ordinate in figure 7.

Tables 10 and 11 present the discrimination parameters for various armor samples. Figures 6 and 7 illustrate the backface signature/animal data as applied to the models.

Table 10. Average Discriminant Parameters for Four-Parameter Model
(.38-Caliber Projectile)

Material	Ply	M	V	W	D	$\ln MV^2$	$\ln WD$
Kevlar 400/2-denier	5	17.67	142.71	40.9	8.65	12.8	5.9
	7	21.32	120.38	48.6	8.93	12.6	6.1
	7(aged)	21.66	120.36	43.4	9.07	12.7	6.0
	9	27.21	91.03	53.4	9.74	12.3	6.2
	15	41.02	61.87	60.6	10.16	12.0	6.4
	23	42.75	59.51	32.6	8.44	11.9	5.6
Kevlar 200-denier	7	14.48	182.04	50.0	8.39	13.1	6.0
Ballistic nylon	12	45.41	56.20	40.4	8.51	11.9	5.8

The use of models such as these in the evaluation of candidate armor materials can be extremely useful. Damage evaluations from animal data when the animals are impacted with the same missiles over the same materials could be graded as to their seriousness. The level of damage could be correlated to a particular volume or depth value obtained from the gelatin studies. When this has been done for a series of materials or plies of material, a relationship could then be constructed from which predictions could be made of the efficiency of candidate armor materials. The net result would be substantially cost effective since fewer animal tests would be required.

V. CONCLUSIONS.

A methodology has been established which provides a nonbiological measure of behind-the-armor effects. This technique, backface signature, utilizes high-speed photography of armor deformation in 20% gel to measure such physical parameters as the volume, depth, and shape of the maximum deformation cavity as well as the deformation time from point of missile impact to cavity formation.

Table 11. Lethality Discriminant Parameters for Eight-Parameter Model*

Goat No.	(Projectile 0.38-Caliber)			Target		Target		Armor type	Lethality	Plot no. symbol
	Mass (M)	Velocity (V)	Diameter (D)	Weight (mass) (W)	Tissue thickness (T)	Lung weight/body weight (L/W)	Arterial O ₂ deviation (AO ₂)	Venous O ₂ deviation (VO ₂)		
	gm	m/sec	mm	kg	cm	gm/kg	%	%		
	Derived from backface signature									
21647	21.32	120.38	89.3	45.8	2.1	10.92	6.2	10.7	Kevlar 7-ply, 400 2-denier	□
21648	21.32	120.38	89.3	51.8	2.5	11.85	8.9	27.0	Kevlar 7-ply, 400 2-denier	
21649	21.32	120.38	89.3	48.4	2.4	10.91	11.9	30.3	Kevlar 7-ply, 400 2-denier	
23015	21.32	120.38	89.3	41.3	2.2	6.92	2.3	30.2	Kevlar 7-ply, 400 2-denier	
23016	21.32	120.38	89.3	44.5	3.1	9.75	4.7	30.2	Kevlar 7-ply, 400 2-denier	
23019	21.32	120.38	89.3	47.5	2.6	7.94	11.5	46.6	Kevlar 7-ply, 400 2-denier	
23020	21.32	120.38	89.3	45.1	3.1	6.19	13.1	14.7	Kevlar 7-ply, 400 2-denier	
23035	21.66	120.36	90.7	45.8	3.0	8.86	23.9	49.2	Kevlar 7-ply, 400 2-denier (aged)	II
23036	21.66	120.36	90.7	34.4	3.3	7.91	30.7	42.2	Kevlar 7-ply, 400 2-denier (aged)	
23039	21.66	120.36	90.7	50.0	3.3	7.24	42.3	45.6	Kevlar 7-ply, 400 2-denier (aged)	
21629	37.77	65.56	97.4	53.4	3.6	9.68	1.7	9.1	Kevlar 9-ply, 400 2-denier	△
23040	14.48	182.04	83.9	48.0	2.8	9.46	25.6	65.8	Kevlar 7-ply, 200denier	▽
23041	14.48	182.04	83.9	52.1	3.0	10.44	16.2	11.0	Kevlar 7-ply, 200denier	
21625	59.66	42.78	85.1	40.4	3.8	14.18	42.0	23.4	Nylon 12-ply	◊

* Clare, Victor R., Lewis, James H., Mickiewicz, Alexander P., and Sturdivant, Larry M.: FBTR-8016, Human Tissue Data Correlation, May 1978.

** Plotted in figure.

Table 11. Summated

Material	Dose IntMV ⁻² (WID)	Response (tissue damage)	
		Int ₁ W ⁻⁸ % AO ₂ % VO ₂	Int ₂ W ⁻⁸ % AO ₂ % VO ₂
5-Ply Kevlar 29, 400 2-denier	8.6	3.2	
7-Ply Kevlar 29, 400 2-denier	8.9 8.8 8.7 8.9 8.8 8.6 8.5	0.6 8.0 8.3 0.7 8.2 8.4 8.1	
7-Ply Kevlar 29, 400 2-denier (aged)	8.8 8.7 8.4	0.2 0.3 0.3	
7-Ply Kevlar 29, 200denier	6.1 6.9	0.5 0.5	
9-Ply Kevlar 29, 400 2-denier	4.8	3.0	
12-Ply ballistic nylon	4.4	0.8	

Backface signature data have been collected for several armor materials; e.g., 5-ply and 7-ply Kevlar 29, 400/2-denier. Limited firings have been conducted on other constructions of armor materials. These data have been used in the provisional lethality discriminant models generated in the Biophysics Division of this laboratory.

VI. RECOMMENDATIONS.

The backface signature parameters cannot be used to evaluate the effectiveness of protective armor until these physical measures are related to the probability that a particular combination would result in a serious or lethal injury. A predictive model relating the physical measures of the backface signature to the physiological effects, particularly in the nonlethal area, would greatly reduce the cost of armor evaluations. At this time, only a limited data base is available, insufficient for developing an overall vulnerability model.

Backface signature work has also indicated that different combinations of soft armor materials may exhibit different dose-response relationships. Various armor materials which are commercially available should be evaluated.

By increasing the data base from which to draw conclusions, the goal of an overall vulnerability model for predicting the effectiveness of soft armor materials could be reached.

APPENDIX
BACKFACE SIGNATURE COMPUTER PROGRAM

```

1*      REAL MSE, MSR
2*      DIMENSION XP(100),YP(100)
3*      DIMENSION X(100), Y(100), TITLE(13)
4*      DIMENSION SM(100)
5*      1000 FORMAT ( 1H1, 19HREGRESSION ANALYSIS
6*      2000 FORMAT (I2 , 13A6 )
7*      2500 FORMAT ( 1H , 13A6 )
8*      3000 FORMAT (2F10.2)
9*      4000 FORMAT (9H      Y = , F10.4 , 3H+ ( , F10.4 , 3H) X      )
10*     4100 FORMAT (9H      Y = , F10.4 , 3H+ ( , F10.4 , 8H)LOG(X)   )
11*     4200 FORMAT (9H LOGY = , F10.4 , 3H+ ( , F10.4 , 8H) X      )
12*     4300 FORMAT (9H LOGY = , F10.4 , 3H+ ( , F10.4 , 8H)LOG(X)   )
13*     4400 FORMAT (9H 1/Y = , F10.4 , 3H+ ( , F10.4 , 8H)LOG(X)   )
14*     4500 FORMAT (9H LOGY = , F10.4 , 3H+ ( , F10.4 , 8H)1/X      )
15*     4600 FORMAT (9H 1/Y = , F10.4 , 3H+ ( , F10.4 , 8H) X      )
16*     4700 FORMAT (9H 1/Y = , F10.4 , 3H+ ( , F10.4 , 8H)1/X      )
17*     4800 FORMAT (9H Y = , F10.4 , 3H+ ( , F10.4 , 8H)1/X      )
18*     4900 FORMAT (5H Y** ,F7.4 , 2H = , F10.2 , 3H+ ( , F10.4 , 5H) X**
19*           1,F7.4   )
20*     5000 FORMAT (1HO, 10X, 14HSTANDARD ERROR ,12X, 1HT,    //)
21*     5500 FORMAT (2H A , 2F20.5 , 5X 15HSIGNIFICANT AT , F6.2 ,
22*           19H PER CENT   )
23*     5600 FORMAT (2H B , 2F20.5 , 5X 15HSIGNIFICANT AT , F6.2 ,
24*           19H PER CENT   )
25*     5700 FORMAT (1H , 20HANALYSIS OF VARIANCE , //, 7H SOURCE , 10X,
26*           12HDF , 10X , 11HMEAN SQUARE , 10X , 1HF ,// )
27*     6500 FORMAT (11H REGRESSION , 6X, 1H1 , 10X , F10.5 , 6X , F10.0 ,
28*           115HSIGNIFICANT AT , F6.2 , 9H PER CENT   )
29*     6600 FORMAT (6H ERROR 8X , I3 , 10X , F10.5 , //, 4H R = ,
30*           1F10.5,4X,15HSIGNIFICANT AT , F6.2 ,9H PER CENT ,// )
31*     7000 FORMAT (1H ,12X,3H X , 10 X 1HY , 10X 9HYESTIMATE ,9X,'Y-YLIST'
32*           1//)
33*     8000 FORMAT (1H ,4F15.5)
34*       1 PY = 1.0
35*       PX=1.0
36*       RX=0.0
37*       WRITE (6,1000)
38*       READ (5,2000) JTYPE, (TITLE(I) , I = 1,13)
39*       WRITE (6,2500) (TITLE(I) , I = 1,13)
40*       WRITE (6,21) JTYPE
41*       21 FORMAT (1H ,I4)
42*       DO 8 I = 1,100
43*       READ (5,3000,END = 9 ) XP(I),YP(I)
44*       8 CONTINUE
45*       9 N = I - 1
46*       IF (JTYPE.NE.-1) GO TO 10

```

```

47*      DO 75 JTYPE = 0,8
48*      10 SX = 0.0
49*          SY = 0.0
50*          SXSQ = 0.0
51*          SYSQ = 0.0
52*          SXY = 0.0
53*          M=0
54*          I=0
55*          IF (JTYPE.NE.9) GO TO 5
56*          READ (5,3000) PX ,PY
57*      5 CONTINUE
58*          I=I+1
59*          X(I) = XP(I)
60*          Y(I) = YP(I)
61*          IF (JTYPE.EQ.0) GO TO 20
62*          GO TO (11,12,13,14,15,16,17,18,19,19),JTYPE
63*      11 X(I) = ALOG10(X(I))
64*          GO TO 20
65*      12 Y(I) = ALOG10(Y(I))
66*          GO TO 20
67*      13 X(I) = ALOG10(X(I))
68*          Y(I) = ALOG10(Y(I))
69*          GO TO 20
70*      14 X(I) = ALOG10(X(I))
71*          Y(I)=1.0/Y(I)
72*          GO TO 20
73*      15 X(I) = 1.0/X(I)
74*          Y(I) = ALOG10(Y(I))
75*          GO TO 20
76*      16 Y(I) = 1.0/Y(I)
77*          GO TO 20
78*      17 X(I) = 1.0/X(I)
79*          Y(I) = 1.0/Y(I)
80*          GO TO 20
81*      18 X(I) = 1.0/X(I)
82*          GO TO 20
83*      19 X(I) = X(I)**PX
84*          Y(I) = Y(I)**PY
85*      20 SY = SY + Y(I)
86*          SX = SX + X(I)
87*          SXSQ = SXSQ + X(I)**2.0
88*          SYSQ = SYSQ + Y(I)**2.0
89*          SXY = SXY + X(I)*Y(I)
90*          M=M+1
91*          IF (M.NE.N) GO TO 5
92*      25 CONTINUE
93*          B = (SXY - (SX*SY/FLOAT(N)))/(SXSQ - (SX*(SX/FLOAT(N))))
94*          A = (SY/FLOAT(N) - B*SX/FLOAT(N))
95*          MSR = (SXY - SX*SY/FLOAT(N))**2.0/(SXSQ - SX**2.0/FLOAT(N))
96*          DF = FLOAT(N) - 2.0
97*          MSE = ((SYSQ - SY**2.0/FLOAT(N)) - MSR)/DF
98*          F = MSR/MSE

```

```

99*      CORR =SQRT(MSR/(SYSQ - SY**2.0/FLOAT(N)))
100*     TR = CORR*SQRT(DF/(1.0 - CORR**2.0))
101*     SEA=SQRT(SXSQ*SEB/FLOAT(N))
102*     SEB = SQRT(MSE/(SXSQ - SX**2.0/FLOAT(N)))
103*     TA = A/SEA
104*     TB = B/SEB
105*     IF (JTYPE.EQ.0) GO TO 40
106*     GO TO (41,42,43,44,45,46,47,48,49,49) ,JTYPE
107*     40 WRITE (6,4000) A,B
108*     GO TO 50
109*     41 WRITE (6,4100) A,B
110*     GO TO 50
111*     42 WRITE (6,4200) A,B
112*     GO TO 50
113*     43 WRITE (6,4300) A,B
114*     GO TO 50
115*     44 WRITE (6,4400) A,B
116*     GO TO 50
117*     45 WRITE (6,4500) A,B
118*     GO TO 50
119*     46 WRITE (6,4600) A,B
120*     GO TO 50
121*     47 WRITE (6,4700) A,B
122*     GO TO 50
123*     48 WRITE (6,4800) A,B
124*     GO TO 50
125*     49 WRITE (6,4900) PY,A,B,PX
126*     50 CONTINUE
127*     WRITE (6,5000)
128*     ABTA = ABS(TA)
129*     ABTB = ABS(TB)
130*     IDF = N- 2
131*     VAR1 = STUD(ABTA,IDF)
132*     VAR1 = 100.0*VAR1
133*     VAR2 = STUD(ABTB,IDF)
134*     VAR2 = 100.0*VAR2
135*     WRITE (6,5500) SEA , TA , VAR1
136*     WRITE (6, 5600) SEB , TB , VAR2
137*     WRITE ( 6, 5700)
138*     TREG = SQRT(F)
139*     VAR3 = STUD(TREG,IDF)
140*     VAR3 = 100.0*VAR3
141*     WRITE (6,6500) MSR , F , VAR3
142*     VAR4 = STUD(TR,IDF)
143*     VAR4 = 100.0*VAR4
144*     WRITE (6,6600) IDF , MSE , CORR , VAR4
145*     WRITE (6,7000)
146*     DO 75 I=1,N
147*     YEST=A+B*X(I)
148*     IF (JTYPE.EQ.0) GO TO 60
149*     GO TO (60,62,62,64,62,64,64,60,69,69,69) , JTYPE
150*     62 YEST = 10.0**YEST

```

```
151*      GO TO 60
152*      64 YEST = 1.0/YEST
153*      GO TO 60
154*      69 IF (YEST.LT.0.0) GO TO 80
155*      YEST=YEST**(1.0/PY)
156*      60 SM(I)=YP(I)-YEST
157*      GO TO 81
158*      80 YEST=0.0
159*      SM(I)=0.0
160*      GO TO 93
161*      81 WRITE (6,8000) XP(I),YP(I),YEST,SM(I)
162*      RRX=SM(I)*SM(I)
163*      RX=RX+RRX
164*      GO TO 75
165*      93 WRITE (6,8000) XP(I),YP(I),YEST, SM(I)
166*      75 CONTINUE
167*      RRXX=RX/N
168*      RMS=SQRT(RRXX)
169*      WRITE (6,97) RMS
170*      VOL=3.141592653*XP(1)*A+(3.141592653/2.0)*B*XP(1)**2
171*      PRINT 98,VOL
172*      98 FORMAT (2X,'VOLUME=',F10.5,1X,'CUBIC CENTIMETERS')
173*      97 FORMAT (///1H , 'RMS = ',F10.5)
174*      GO TO 1
175*      END
```

```

1*      DIMENSION DIAMY(20),DEPTHX(20),XNEW(20),YNEW(20),CXNEW(20),
2*      1CYNEW(20),COD(20),COW(20),V(20)
3*      DIMENSION TITLE(10)
4*      READ 7,JTYPE,(TITLE(I),I=1,10)
5*      PRINT 8,(TITLE(I),I=1,10)
6*      READ 1,M,N,X,Y,PPS
7*      C      M=REPRSEENTS THE NO. OF FRAME COUNTS TO MAX. DEPTH
8*      C      N=REPRSEENTS THE NO. OF DIAMETERS MEASURED FROM MAX DEPTH
9*      READ 2,(DEPTHX(I),I=1,M)
10*     READ 2,(DIAMY(I),I=1,N)
11*     PRINT 9,(DEPTHX(I),DIAMY(I),I=1,N)
12*     1 FORMAT(5X,I2,5X,I2,5X,F4.0,5X,F4.05X,F5.0)
13*     2 FORMAT(16F5.0)
14*     CX=10.0/X
15*     CY=4.0/Y
16*     DO 10 I=1,M
17*     10 COD(I)=DEPTHX(I)*CX
18*     DO 20 I=1,N
19*     20 COW(I)=DIAMY(I)*CY
20*     XINC=DEPTHX(M)/10.0
21*     XNEW(1)=DEPTHX(M)
22*     J=0
23*     DO 30 I=1,10
24*     K=N-J
25*     J=J+1
26*     XNEW(I)=DEPTHX(M)-(FLOAT(I-1)*XINC)
27*     30 YNEW(I)=DIAMY(K)
28*     DO 40 I=1,10
29*     40 CXNEW(I)=XNEW(I)*CX
30*     40 CYNEW(I)=YNEW(I)*CY/2.0
31*     DO 50 I=1,M
32*     50 V(I)=(COD(I)-COD(I-1))*PPS*10**-2
33*     TIME=FLOAT(M)*(1.0/PPS)
34*     PRINT 3,M,N,X,Y,XINC,PPS
35*     PRINT 4,(CXNEW(I),CYNEW(I),I=1,10)
36*     PRINT 5,V(1),TIME
37*     PRINT 5,(V(I),I=2,M)
38*     3 FORMAT( )
39*     PRINT 12,(COD(I),COW(I),I=1,N)
40*     12 FORMAT('0',3X,'DEPTH CONVERSION',10X,'WIDTH CONVERSION',//(3X,
41*           1F8.4,10X,F8.4))
42*     4 FORMAT('0',3X,'X',10X,'Y',//(F8.4,3X,F8.4))
43*     5 FORMAT('0',3X,'VELOCITY',10X,'TIME',//(3X,F8.4,10X,F8.4))
44*     6 FORMAT(3X,F8.4)
45*     7 FORMAT(I2,10A6)
46*     8 FORMAT('1',2X,'FILM NUMBER',2X,10A6)
47*     9 FORMAT(2X,'RAW VALUES FOR TEST MATRIX',//(2X,F10.5,2X,F10.5))
48*     11 FORMAT(2F10.2)
49*     WRITE(7,7) JTYPE,(TITLE(I),I=1,10)
50*     WRITE(7,11) (CXNEW(I),CYNEW(I),I=1,10)
51*     CONTINUE
52*     STOP
53*     END

```

DISTRIBUTION LIST NO. 20

Names	Copies	Names	Copies
EDGEWOOD ARSENAL		Director	
TECHNICAL DIRECTOR		Defense Civil Preparedness Agency	
Attn: SAREA-TD-E	1	Attn: RE(DEP)	1
FOREIGN INTELLIGENCE OFFICER	1	Attn: PO(DC)	1
CHIEF, LEGAL OFFICE	1	Washington, DC 20301	
CHIEF, SAFETY OFFICE	1	US Army Standardization Group, Canada	1
CDR, US ARMY TECHNICAL ESCORT CENTER	1	National Defense Headquarters	
PUBLIC HEALTH SERVICE LO	3	Ottawa, Ontario, Canada K1A-OK2	
AUTHOR'S COPY, Biomedical Laboratory	3	US Army Standardization Group (UK)	
DIRECTOR OF BIOMEDICAL LABORATORY	1	Attn: OCRDA (DAMA-PPI)	1
Attn: SAREA-BL-M	1	Box 65, FPO New York 09510	
Attn: SAREA-BL-B	1	OFFICE OF THE SURGEON GENERAL	
Attn: SAREA-BL-BS	1	Commander	
Attn: SAREA-BL-BW/Mr. N. Montanarelli	31	US Army Research Institute of	
Attn: SAREA-BL-E	1	Environmental Medicine	
Attn: SAREA-BL-H	1	Attn: SGRD-UE-CA	1
Attn: SAREA-BL-V	1	Natick, MA 01760	
DIRECTOR OF CHEMICAL LABORATORY	1	US ARMY HEALTH SERVICE COMMAND	
Attn: SAREA-CL-P	1	Commander	
DIRECTOR OF MANUFACTURING TECHNOLOGY	1	US Army Institute of Surgical Research	
Attn: SAREA-MT-CT	1	Brooke Army Medical Center	
FORT SAM HOUSTON, TX 78234		Fort Sam Houston, TX 78234	
DIRECTOR OF PRODUCT ASSURANCE	1	Superintendent	
Attn: SAREA-PA-A	1	Academy of Health Sciences	
Attn: SAREA-PA-P	1	US Army	
DIRECTOR OF TECHNICAL SUPPORT	2	Attn: HSA-CDC	1
Attn: SAREA-TS-R	2	Attn: HSA-RHE	1
Attn: SAREA-TS-L	3	Fort Sam Houston, TX 78234	
DEPARTMENT OF DEFENSE		US ARMY MATERIEL COMMAND	
Administrator		Commander	
Defense Documentation Center		US Army Materiel Command	
Attn: Accessions Division	12	Attn: AMCSF-C	1
Cameron Station		Attn: AMCRD-WB	1
Alexandria, VA 22314		Attn: AMCRD-T (Dr. D. Stefanye)	1
5001 Eisenhower Ave		Alexandria, VA 22333	
Director		Commander	
Defense Intelligence Agency		USAMC STIT-EUR	
Attn: DIADI-3H1	1	APO New York 09710	
Attn: DIADI-5C4	1	Redstone Scientific	
Washington, DC 20301		Information Center	
Attn: Chief, Documents		Attn: US Army Missile Command	
DEPARTMENT OF THE ARMY		Redstone Arsenal, AL 35809	2
HQDA (DAMO-ODC)	1		
WASH DC 20310			

DISTRIBUTION LIST NO. 20 (Contd)

Names	Copies	Names	Copies
Commander US Army Science & Technology Center-East Office APO San Francisco 96328	1	CDR, APG Attn: STEAP-TL APG-Aberdeen Area	1
AMC Program Manager for Demilitarization of Chemical Material Attn: AMXDC APG-Edgewood Area	1	US MARINE CORPS	
US ARMY ARMAMENT COMMAND		Director, Development Center Marine Corps Development & Education Command Attn: Ground Operations Division Quantico, VA 22134	1
Commander US Army Armament Command Attn: AMSAR-ASH Attn: AMSAR-RDT Rock Island, IL 61201	1	DEPARTMENT OF THE AIR FORCE	
Commander Rocky Mountain Arsenal Attn: SARRM-EA Attn: SARRM-MD Denver, CO 80240	1	HQ Foreign Technology Division (AFSC) Attn: PDTR-3 Wright-Patterson AFB, OH 45433	1
Commander Frankford Arsenal Attn: Library Branch, TSP-L Bldg 51-2 Philadelphia, PA 19137	1	Director Air Force Inspection and Safety Center Attn: IGD(AFISC/SEV) Norton AFB, CA 92409	1
US ARMY TRAINING & DOCTRINE COMMAND		Commander Armament Development & Test Center Attn: DLOSL (Technical Library) Eglin AFB, FL 32542	1
Commandant US Army Infantry School Brigade & Battalion Operations Department Combat Support Group Attn: NBC Committee Fort Benning, GA 31905	1	HQ, NORAD/DOCUN Ent AFB, CO 80912	1
Commander US Army Institute for Military Assistance Attn: ATSU-CTD-MO Fort Bragg, NC 28307	1	OUTSIDE AGENCIES	
Commander US Army Infantry School Attn: ATSH-CD-MS-C Fort Benning, GA 31905	1	Battelle, Columbus Laboratories Attn: TACTEC 505 King Avenue Columbus, OH 43201	1
US ARMY TEST & EVALUATION COMMAND		ADDED ADDRESSEES	
Record Copy CDR, APG Attn: STEAP-AD-R/RHA APG-Edgewood Area, Bldg ES179	1	US Department of Justice Law Enforcement Assistance Administration Attn: Mr. Lester D. Shubin 633 Indiana Ave WASH DC	15